

An Improved Algorithm for Selecting Ground Motions to Match a Conditional Spectrum

Jack W. Baker and Cynthia Lee

Department of Civil & Environmental Engineering, Stanford University, USA

This paper describes an algorithm to efficiently select ground motions from a database while matching a target mean, variance and correlations of response spectral values at a range of periods. The approach improves an earlier algorithm by Jayaram et al. (2011). Key steps in the process are to screen a ground motion database for suitable motions, statistically simulate response spectra from a target distribution, find motions whose spectra match each statistically simulated response spectrum, and then perform an optimization to further improve the consistency of the selected motions with the target distribution. These steps are discussed in detail, and the computational expense of the algorithm is evaluated. A brief example selection exercise is performed, to illustrate the type of results that can be obtained. Source code for the algorithm has been provided, along with metadata for several popular databases of recorded and simulated ground motions, which should facilitate a variety of exploratory and research studies.

1 Introduction

Selection of ground motions is a topic of great interest as dynamic structural analysis, which requires ground motions as inputs, grows more prevalent (Katsanos et al. 2010; NIST 2011). This selection typically involves searching a ground motion database to find time series produced under appropriate seismological conditions (e.g., earthquake magnitude and source-to-site distance), and that have appropriate response spectral values. In some cases, ground motions are selected based on their individual match to a target spectrum; that is, an optimal set of ground motions would have spectra that all perfectly match the target spectrum. In other cases, however, it is important that the ground motions have variability in response spectra that accurately represents target distributions from predictive models (e.g., Kramer and Mitchell 2006; Lin et al. 2013b). As such, a number of algorithms have been proposed to select ground motions with some form of specified response spectral variability (Bradley 2012; Ha and Han 2016a; b; Jayaram et al. 2011; Kottke and Rathje 2008; Wang 2011). Among those algorithms, only

31 Bradley, Ha and Han (2016b) and Jayaram et al. include two features of interest here: accounting
32 for correlations among spectral parameters and conditioning on a target spectral acceleration
33 amplitude.

34 Traditional practice in active seismic regions has been to search databases of ground motion
35 recordings, but simulated ground motions are receiving increased use. Further, there is a need for
36 comparative research studies where recorded and simulated motions are selected in a comparable
37 manner and their relative impacts on structures are evaluated (e.g., Galasso et al. 2013; Iervolino
38 et al. 2010). In recognition of these trends, data facilitating searches of several popular libraries
39 of recorded and simulated ground motions are provided with this algorithm. A second trend in
40 ground motion libraries is that they are rapidly growing larger (several databases discussed
41 below have more than 10,000 ground motions), making the computational efficiency of search
42 algorithms more important.

43 This manuscript describes an updated version of the algorithm proposed by Jayaram et al.
44 (2011), also utilizing aspects of Bradley (2012). Relative to the Jayaram et al. algorithm, the
45 range of selection options has been broadened and the numerical implementation has been
46 improved to both reduce runtime and improve the statistics of the resulting selected motions.
47 Improvements relative to the previous algorithm are noted below, and improvements in
48 numerical efficiency are also reported.

49 **2 Target Response Spectra**

50 **2.1 Types of Spectral Targets**

51 Before discussing the ground motion selection procedure, we first introduce some relevant
52 terminology and concepts related to response spectra as targets for ground motion selection.
53 Ground motion models (GMMs) (e.g., Boore et al. 2014) provide the mean and standard
54 deviation of logarithmic spectral acceleration (Sa) at a given period, denoted here as $\mu_{\ln Sa}(Rup, T)$
55 and $\sigma_{\ln Sa}(Rup, T)$, respectively. With this notation, μ denotes a mean, and σ denotes a standard
56 deviation, of the variable noted in subscript. Rup denotes the rupture scenario (defined by the
57 earthquake's magnitude, distance, rupture mechanism, and other parameters necessary to
58 evaluate a given GMM) and T denotes the spectral acceleration period. The GMM prediction
59 also generally depends upon one or more parameters defining site conditions such as average
60 shear-wave velocity over the top 30 m of the site (V_{s30}), but that explicit dependence is omitted
61 from this notation for brevity. Some GMMs (e.g., Abrahamson et al. 2014) also provide

62 correlation coefficients for log spectral accelerations at pairs of periods, denoted here as
 63 $\rho(T_i, T_j)$. If not provided by the GMM, the correlation coefficients can be obtained from a
 64 supplemental model (e.g., Baker and Jayaram 2008).

65 With the above inputs, we define an “Unconditional Spectrum” as the probability distribution
 66 of a response spectrum, given a rupture scenario. The distribution of log spectral acceleration
 67 values at multiple periods, given a rupture, is well represented by a multivariate normal
 68 distribution (Jayaram and Baker 2008), which is fully specified by the mean and covariance
 69 matrix for $\ln Sa$ values

$$70 \quad \mathbf{M} = [\mu_{\ln Sa}(Rup, T_1) \ \mu_{\ln Sa}(Rup, T_2) \ \dots \ \mu_{\ln Sa}(Rup, T_p)]^T \quad (1)$$

$$71 \quad \Sigma = \begin{bmatrix} \sigma_{T_1}^2 & \sigma_{T_1, T_2} & \dots & \sigma_{T_1, T_p} \\ \sigma_{T_2, T_1} & \sigma_{T_2}^2 & & \vdots \\ \vdots & & \ddots & \\ \sigma_{T_p, T_1} & \dots & & \sigma_{T_p}^2 \end{bmatrix} \quad (2)$$

72 where \mathbf{M} is a vector of mean values of $\ln Sa$ at p periods of interest, superscript T denotes a
 73 matrix transpose, and Σ is the covariance matrix for $\ln Sa$ at these same periods. In equation 2
 74 we adopt abbreviated notation, $\sigma_{T_i, T_j} = \rho(T_i, T_j) \sigma_{\ln Sa}(Rup, T_i) \sigma_{\ln Sa}(Rup, T_j)$, to denote the covariance
 75 of $\ln Sa$ at periods T_i and T_j (and $\sigma_{T_i}^2 = \sigma_{\ln Sa}(Rup, T_i)^2$ is the variance at period T_i).

76 The “Unconditional” terminology is used here to emphasize the lack of conditioning on a
 77 spectral value, for consistency with the use of the term “Conditional” in the following two
 78 definitions. An example Unconditional Spectrum is illustrated in Figure 1a. The mean value
 79 from equation 1, and the standard deviations embedded in equation 2, are plotted in Figure 1a;
 80 the period-to-period correlation embedded in equation 2 is apparent in the ground motion spectra
 81 plotted in the figure, which are ‘bumpy’ (reflecting a lack of perfect correlation) but do vary with
 82 some continuity from period to period.

83 The “Conditional Mean Spectrum” (CMS) quantifies mean log spectral acceleration values
 84 of a ground motion, conditional on a spectral value at a conditioning period and a rupture
 85 scenario

$$86 \quad \mu_{\ln Sa(T_i) | \ln Sa(T^*)} = \mu_{\ln Sa}(Rup, T_i) + \rho(T_i, T^*) \varepsilon(T^*) \sigma_{\ln Sa}(Rup, T_i) \quad (3)$$

87 where T^* denotes the conditioning period and $\varepsilon(T^*)$ is a residual quantifying the difference
 88 between the conditioning Sa value ($Sa(T^*)$) and its mean value given the considered rupture

$$89 \quad \varepsilon(T^*) = \frac{\ln Sa(T^*) - \mu_{\ln Sa}(Rup, T^*)}{\sigma_{\ln Sa}(Rup, T^*)} \quad (4)$$

90
 91 A CMS, as calculated using equation 3 and a conditioning period of 1.5s, is illustrated in Figure
 92 1b. The term CMS was introduced by Baker and Cornell (2006), and further background is
 93 provided in Baker (2011). It is becoming more commonly used to select ground motions for
 94 dynamic analysis in several design guidelines (e.g., BSSC 2015; FEMA 2012; TBI Guidelines
 95 Working Group 2010).

96 The “Conditional Spectrum” (CS) is the probability distribution of log spectral acceleration
 97 values, conditional on a spectral value at a conditioning period and on a rupture scenario. Unlike
 98 the CMS, this spectrum quantifies variability in spectral values at periods other than the
 99 conditioning period. If we assume that the distribution is multivariate normal (which is generally
 100 reasonable), then the Conditional Spectrum is fully described by conditional means, and a
 101 conditional covariance matrix. The conditional means are given by equation 3 and the
 102 conditional covariance matrix is

$$103 \quad \Sigma_{cond} = \Sigma - \frac{\Sigma_{cross} \Sigma_{cross}^T}{\sigma_{\ln Sa}(Rup, T^*)^2} \quad (5)$$

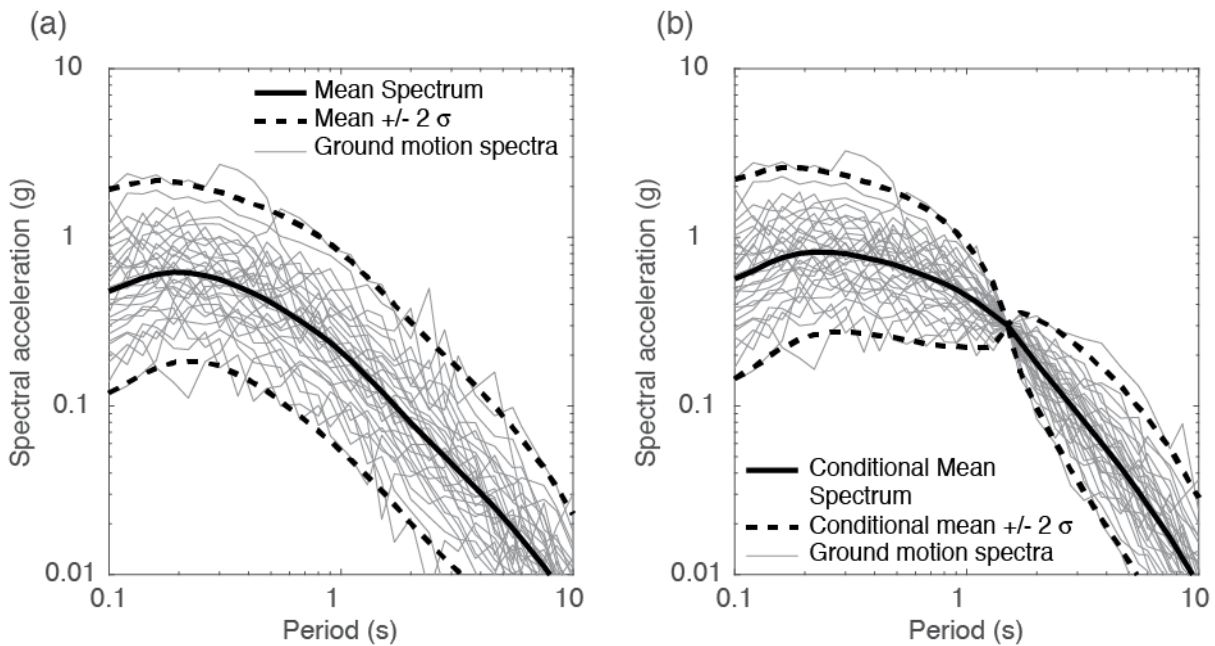
104 where Σ is the covariance matrix from equation 2 and Σ_{cross} is a $p \times 1$ matrix of covariances
 105 between $\ln Sa(T_i)$ and $\ln Sa(T^*)$. Visually we can represent this distribution by plotting the mean
 106 and +/- one or two standard deviations around the mean, as in Figure 1b. The Conditional
 107 Spectrum terminology was coined by Abrahamson and Al Atik (2010), but they represented the
 108 CS distribution directly by realizations of the spectra rather than an analytical distribution. The
 109 Conditional Mean Spectrum was more popular than the Conditional Spectrum prior to
 110 approximately 2010, in large part because there was no simple way to select ground motions
 111 matching a Conditional Spectrum—a situation rectified by this manuscript and its predecessor
 112 algorithms.

113 Bradley (2010) extended the CS to consider ground motion parameters other than response
 114 spectra, and to consider a more general situation where more than one rupture scenario may
 115 contribute to occurrence of ground motions with the target amplitude. Bradley refers to the

116 resulting distribution and selection procedure as a Generalized Conditional Intensity Measure
117 (GCIM) approach. This paper focuses on response spectra and single rupture scenarios for
118 simplicity, but the algorithm could, in principle, be generalized by defining equations 3 and 5 to
119 refer to a general vector of intensity measures and to reflect the impact of multiple rupture
120 scenarios on the target means and covariances. Equations 3 and 5 can also be revised to account
121 for the use of multiple GMMs, consistent with current practice in hazard analysis (Lin et al.
122 2013a).

123 To complement the above equations, a few observations may provide intuition about the
124 Conditional Spectrum target illustrated in Figure 1b. First, the response spectra “pinch” to a
125 single point at the conditioning period of 1.5s. Since we have specified this amplitude, there is no
126 variability in the spectra at this period. Second, at other periods there is variability in the spectra
127 and that variability tends to be larger at periods further from 1.5s. This is a result of the
128 correlation between spectral values: periods close to 1.5s have spectra highly correlated to
129 $Sa(1.5s)$, so there is relatively little uncertainty in spectra at these nearby periods, while there is
130 larger spectral variability at the (less-correlated) periods far from 1.5s. This pattern in spectral
131 variability is grossly similar to what is observed if one simply scales a set of ground motions so
132 their spectra are equal at some conditioning period, which somewhat confirms the
133 reasonableness of this target. Third, the mean of the conditional spectrum (i.e., the CMS) reflects
134 the expected response spectral shape, and it accounts for both the spectrum associated with the
135 rupture scenario (via the unconditional mean spectrum of equation 1) and the tendency for high-
136 amplitude spectral values to be associated with a peak in the spectrum (via the epsilon value and
137 spectral correlations in equation 3).

138 It should be intuitive that mean responses obtained from structural analysis are related to the
139 mean amplitude of the input ground motions’ spectra. Further, several studies have shown that
140 considering the full variability in response spectra, rather than only mean values of spectra, can
141 be important for some structural response assessment procedures (e.g., Lin et al. 2013b). This
142 motivates the development of tools like that proposed here to facilitate selection of ground
143 motions matching an Unconditional Spectrum or Conditional Spectrum.



144
 145 Figure 1. (a) Unconditional Spectrum associated with magnitude = 6.5, distance = 10 km, $V_{s30} = 500$ m/s
 146 and a California strike-slip rupture. (b) Conditional spectrum associated with the same rupture parameters
 147 as (a), and with $Sa(1.5s) = 0.3$ g. Response spectra consistent with the target distributions are also shown.
 148 Calculations use the GMM of Boore et al. (2014) and the correlation model of Baker and Jayaram (2008).

149 2.2 Computational Challenges

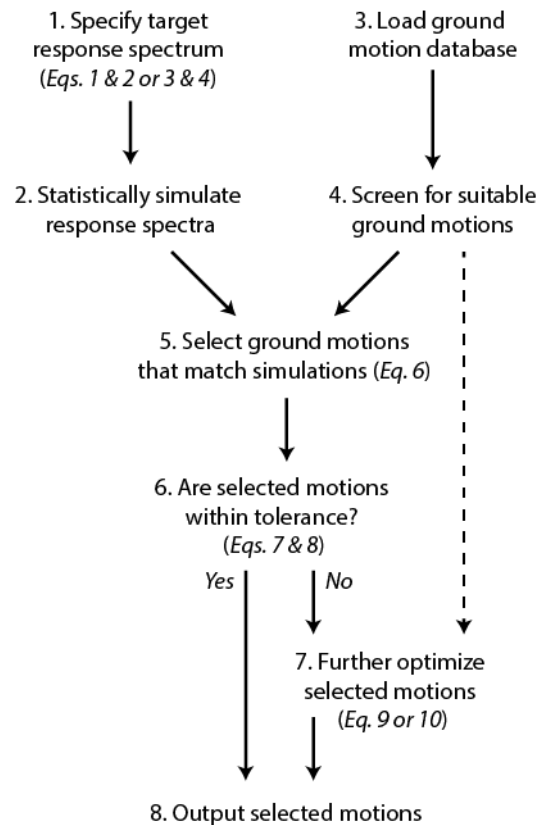
150 With the above methods for quantifying response spectra targets established, here we briefly
 151 consider ground motion selection strategies (thinking of the case where one wishes to select n
 152 ground motions from a database with m candidate motions). It is simple to quickly select ground
 153 motions to be consistent with a Conditional Mean Spectrum, as only a mean spectrum is
 154 relevant: one can simply compute an error metric for each of the m candidate motions (e.g., the
 155 sum of squared errors between the ground motion’s spectrum and the target spectrum, potentially
 156 after scaling the motion), and then selects the n motions with the smallest error. There may be a
 157 benefit to performing a more extensive optimization-based search as discussed below, but the
 158 availability of this fast approach makes the optimization-based approach less critical.

159 It is much more difficult to select ground motions that match a Conditional Spectrum or
 160 Unconditional Spectrum target, because the ground motions’ spectra should match both a mean
 161 target and a covariance matrix. To find ground motions with an appropriate covariance matrix,
 162 one cannot evaluate individual candidates but instead must evaluate a set of n candidates
 163 collectively (that is, it is not possible to determine whether an individual ground motion is a
 164 “good” fit to a Conditional Spectrum without knowing the other ground motions it would be
 165 paired with). This means that there are m -choose- n combinations of ground motions to

166 consider—too many to search exhaustively for typical situations where $n > 10$ and $m > 100$. It is
167 this problem that the algorithm below addresses, via heuristics to enable a fast search that
168 consistently produces ground motion sets closely matching the specified targets.

169 3 Selection Algorithm

170 The major steps of the proposed ground motion selection process are illustrated in Figure 2.
171 These steps are described in additional detail in the following subsections, which group the steps
172 into distinct conceptual stages.



173
174

175 Figure 2. Flow chart of major steps in the ground motion selection process, with relevant equation
176 numbers noted in parantheses. Details for each step are discussed in Section 3.

177 3.1 Compute Target Spectrum and Statistically Simulate Realizations

178 The process starts by specifying a target response spectrum (Step 1 in Figure 2). Formally,
179 we specify the mean values of log spectral acceleration, and the covariance matrix for these
180 values. Equations 1 and 2 are utilized if the target is an Unconditional Spectrum, and equations 3
181 and 5 are utilized if the target is a Conditional Spectrum. The provided software includes a
182 function that computes the required mean and covariance matrix if the user specifies the target
183 earthquake rupture (and the target $\epsilon(T^*)$ or $Sa(T^*)$ if the target is a Conditional Spectrum). The

184 provided software utilizes the models of Boore et al. (2014) and Baker and Jayaram (2008) to
185 compute the target spectra, but these can be replaced without significant modification to the code
186 if desired.

187 While the software was developed to solve the problem of selecting ground motions to match
188 a Conditional Spectrum, it can also be adopted for selecting ground motions to match a code
189 spectrum or some other target, by specifying the target spectrum as the mean spectrum, and
190 setting the covariance matrix to consist of all zeros (i.e., specifying that no variability around the
191 target spectrum is desired).

192 Relative to Jayaram et al. (2011), there are a few updates to the target response spectrum
193 calculation. The main program has been generalized so that a single function can handle
194 Conditional Spectrum and Unconditional Spectrum targets (previously, separate versions of the
195 software were provided for each target type). Additionally, functionality has been provided so
196 that the user can easily match a target $Sa(T^*)$ with a given set of rupture values. Because mean
197 rupture values (rather than the full distribution of possible ruptures considered in a seismic
198 hazard calculation) are often used in these calculations for convenience, the target $Sa(T^*)$ is not
199 necessarily obtained when these mean values are combined with a mean $\varepsilon(T^*)$ value from a
200 hazard deaggregation. An optional calculation now adjusts the $\varepsilon(T^*)$ value so that the
201 conditional mean spectrum matches the target $Sa(T^*)$, as this was seen by Lin et al. (2013) to be
202 a reasonable approximation strategy in many cases.

203 Step 2 in Figure 2 is to statistically simulate realizations of response spectra from the target
204 distribution. This is done by sampling from a multivariate normal distribution with the target
205 mean and covariance matrices. Since this simulation step is extremely fast, it is performed
206 multiple times and the set of simulations best matching the target spectrum is utilized for the
207 following steps. We note here that the ‘statistically simulated spectra’ in this step are produced
208 by sampling from a probability distribution (e.g., Stein 1987); this is distinct from the ‘simulated
209 ground motions’ discussed in the following section, where are produced by numerical evaluation
210 of equations associated with the earthquake rupture and seismic wave propagation process.

211 **3.2 Specify Candidate Ground Motions**

212 Step 3 of the process in Figure 2 specifies candidate ground motions to select from. Relevant
213 metadata from a candidate ground motion database is loaded, including spectral acceleration
214 values and rupture parameters for each ground motion. The Jayaram et al. (2011) code included

215 metadata for the NGA-West1 database, consisting of 3551 ground motions from 173 earthquakes
216 (Chiou et al. 2008). Here we have added metadata for the NGA-West2 database, which includes
217 21,539 ground motions from 599 earthquakes (Ancheta et al. 2014). Additionally, we have added
218 metadata for three databases of numerically simulated ground motions produced by a Southern
219 California Earthquake Center (SCEC) project to validate simulations (Goulet et al. 2015).
220 Simulations were produced on the SCEC Broadband Platform using rupture geometries from
221 seven recent California earthquakes. Ground motions from the “EXSIM” (Atkinson and
222 Assatourians 2015), “GP” (Graves and Pitarka 2015) and “SDSU” (Olsen and Takedatsu 2015)
223 simulation algorithms were compiled for use in this software. Each database includes 13,400
224 ground motions. Because both recorded and simulated ground motion databases are provided in a
225 compatible format, the authors hope that this tool will facilitate further comparative evaluations
226 of similarities and differences in structural demands caused by recorded versus simulated ground
227 motions with comparable response spectra.

228 An additional improvement in Steps 2 and 3 of the selection process is that the new target
229 computations and ground motion databases utilize both the RotD50 and RotD100 direction-
230 independent metrics of response spectra for multi-component motions (Boore 2010). These
231 metrics are now used often in ground motion models and engineering analysis procedures
232 (Stewart et al. 2011), so their inclusion in the database metadata increases the tool’s relevance.
233 Single-component response spectra are also provided so that users can search for single-
234 component motions if desired.

235 Once database metadata has been loaded, it is screened in Step 4 so that only appropriate
236 ground motions are considered for selection. The current code is set up to allow only ground
237 motions with appropriate values of earthquake magnitude, source-to-site distance, and V_{s30} , but
238 the screening can be easily generalized to consider other properties. These so-called causal
239 parameters are important to screen in order to assure that the considered time series are
240 reasonably consistent with the conditions of interest in ground motion selection, but they should
241 not be screened so aggressively that an insufficient number of candidate motions remain for the
242 next stage of selection (Tarbali and Bradley 2016). The Jayaram et al. (2011) code did not
243 include this screening step, as its objective was to illustrate other aspects of the selection
244 procedure, but the screening has been added here both to improve the quality of the selected
245 motions and to improve the computational cost of the calculation (since motions excluded at this
246 stage need not be considered later for selection).

247 **3.3 Ground Motion Selection**

248 Step 5 of Figure 2 involves selecting ground motions from the database that best match the
 249 statistically simulated spectra. For each statistically simulated spectrum and candidate ground
 250 motion, the sum of squared errors (*SSE*) is computed

$$251 \quad SSE = \sum_{j=1}^P \left(\ln S_a(T_j) - \ln S_a^{(s)}(T_j) \right)^2 \quad (6)$$

252 where $\ln S_a(T_j)$ is the log spectral acceleration of the (optionally scaled) candidate ground
 253 motion and $\ln S_a^{(s)}(T_j)$ is the $\ln S_a$ of the considered statistically simulated response spectrum.
 254 Note that if scaling is not allowed and a target Conditional Spectrum is used, the selected
 255 motions will not exactly match the target $Sa(T^*)$, but equation 6 will encourage selection of
 256 motions close to the target and the motions may be suitably similar if choosing from a database
 257 having ground motions compatible with the target scenario. For each statistically simulated
 258 spectrum, the *SSE* is computed for all candidate ground motions that have not already been
 259 selected, and the motion with the smallest *SSE* is selected to represent that simulation. The
 260 metric of equation 6 is not the only possible selection criterion (e.g., Beyer and Bommer 2007;
 261 Buratti et al. 2010), but has been observed to produce satisfactory results; it could easily be
 262 modified by a user if desired (e.g., to put varying weights on the squared errors at varying
 263 periods).

264 Simulating spectra from the target distribution (in Step 2), and then searching individual
 265 motions to find matches to these simulations, is perhaps the most important step in this algorithm
 266 for overcoming the computational cost that would be required to search suites of ground motions
 267 instead of individual motions. Its utility is apparent when noting that most prior algorithms to
 268 solve this problem have used this approach (Bradley 2012; Jayaram et al. 2011; Wang 2011),
 269 though Ha and Han (2016a) recently proposed a non-simulation-based approach that instead uses
 270 a limited search of the potential selection combinations.

271 In Step 6 of Figure 2, the selected suite of motions is evaluated to see whether it is
 272 sufficiently close to the target distribution. The maximum percentage mismatch of the mean and
 273 standard deviation of the selected motions' spectra, relative to their targets, are calculated

$$274 \quad Err_{mean} = \max_j \left(\frac{|m_{\ln Sa}(T_j) - \mu_{\ln Sa}(T_j)|}{\mu_{\ln Sa}(T_j)} \right) \times 100 \quad (7)$$

275
$$Err_{std} = \max_j \left(\frac{|s_{\ln Sa}(T_j) - \sigma_{\ln Sa}(T_j)|}{\sigma_{\ln Sa}(T_j)} \right) \times 100 \quad (8)$$

276 where $m_{\ln Sa}(T_j)$ is the sample mean of the $\ln Sa$ values of the selected motions at period T_j and
 277 $\mu_{\ln Sa}(T_j)$ is the target mean from a GMM (in the case of Unconditional Selection) or equation 5
 278 (in the case of Conditional Selection). Similarly, $s_{\ln Sa}(T_j)$ is the sample standard deviation and
 279 $\sigma_{\ln Sa}(T_j)$ is the target standard deviation at period T_j . Finally, $| \cdot |$ denotes an absolute value. The
 280 user can specify a maximum tolerance for the errors defined by equations 7 and 8, and if the
 281 errors at this step are less than the tolerance then the selection process is complete.

282 If the errors are too large, then a finite number of optimization rounds are performed to
 283 further improve the selection. Step 7 of Figure 2 involves further optimizing the initial selection
 284 if needed. At this stage, the selected set of ground motions are modified by replacing individual
 285 ground motions from the set with available motions from the screened database and seeing
 286 whether the set is improved in its match to the target response spectrum. There are two objective
 287 functions available to the user when performing the optimization.

288 In the first case, a weighted sum (over all periods of interest) of squared errors in the
 289 spectra's mean values and standard deviations are utilized to evaluate goodness of fit, as follows

290
$$SSE_s = \sum_{j=1}^p \left[\left(m_{\ln Sa}(T_j) - \mu_{\ln Sa}(T_j) \right)^2 + w \left(s_{\ln Sa}(T_j) - \sigma_{\ln Sa}(T_j) \right)^2 \right] \quad (9)$$

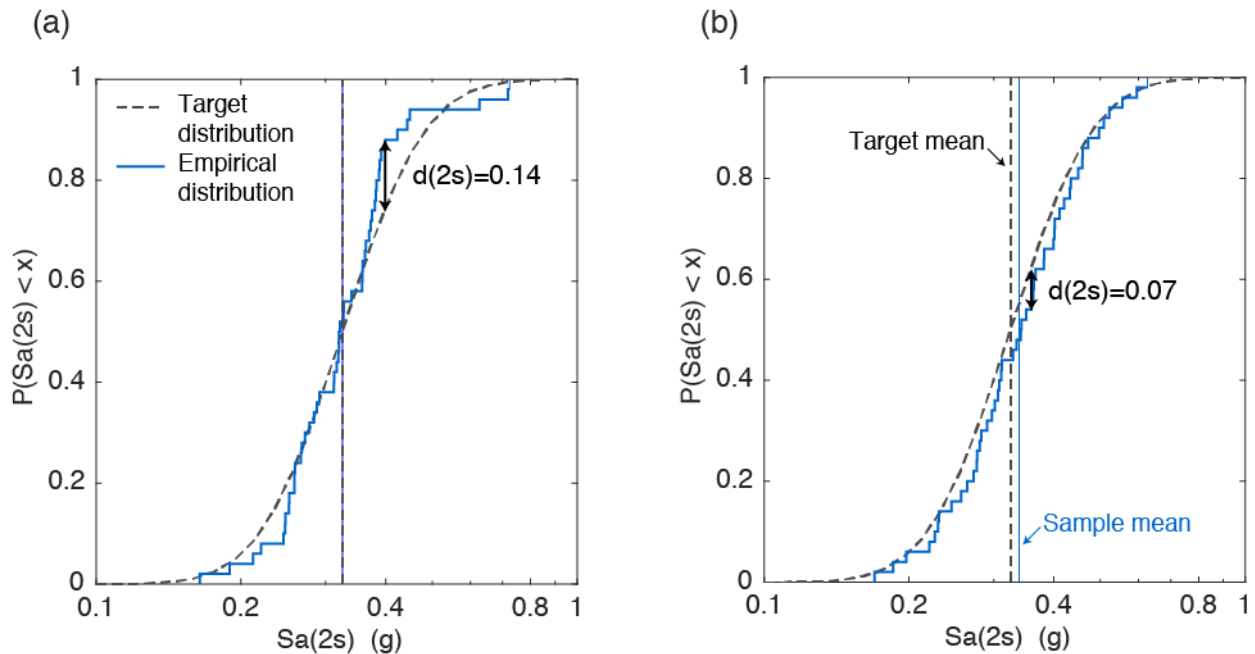
291 where SSE_s denotes the sum of squared errors of the set of ground motions, w is a user-defined
 292 weight that assigns relative importance to mismatches in mean versus standard deviation values.

293 In the second case, the d statistic from a Komogorov-Smirnov goodness of fit test (KS test) is
 294 used as the metric. The d statistic at a given period is given by the maximum absolute values of
 295 the difference between the target distribution's cumulative distribution function ($F_{\ln Sa(T_j)}(x)$)
 296 and the empirical cumulative distribution function ($F_{\ln Sa(T_j)}^*(x)$) given by the selected motions'
 297 $Sa(T_j)$ values

298
$$d(T_j) = \max \left(\left| F_{\ln Sa(T_j)}^*(x) - F_{\ln Sa(T_j)}(x) \right| \right) \quad (10)$$

299 Example d values are illustrated in Figure 3 for a single period. In the software, the d values for
 300 all periods of interest are summed and used as the error metric. This metric has been successfully
 301 utilized by others in ground motion selection problems (Bradley 2012; Chandramohan et al.
 302 2016), and so is incorporated into this algorithm to take advantage of this insight.

303 Figure 3 illustrates the implications of these error metrics using a target distribution for
 304 $Sa(2s)$, and $Sa(2s)$ values for two hypothetical sets of candidate ground motions. The target and
 305 sample means are labeled on each figure, as well as the $d(2s)$ value; sample standard deviations
 306 (the third parameter used in error computations) are not shown. In Figure 3a, the candidate
 307 motions have nearly the same mean and standard deviation as the target spectrum, and a $d(2s)$
 308 value of 0.14. In Figure 3b the candidate ground motions have a sample mean that is 4% larger
 309 than the target mean (and, although not shown graphically, the sample standard deviation closely
 310 matches the target). However, the $d(2s)=0.07$ value in this case is half of that in Figure 3a. So the
 311 SSE_S error metric would prefer the motions in Figure 3a while the KS test metric would prefer
 312 the motions in Figure 3b (keeping in mind that the selection algorithm sums errors across
 313 multiple periods rather than considering only a single period as we have here). An additional
 314 relevant factor is that the KS test calculation is somewhat slower than the SSE_S calculation, as
 315 will be seen below. Ultimately it is left to the user to select a metric for a given selection case, as
 316 both error metrics have merits.



317
 318 Figure 3. Illustration of spectral acceleration target distributions and error metrics. (a) Selected ground
 319 motions whose mean and standard deviation closely match the target. (b) Selected ground motions whose

320 mean is slightly less than the target mean, but who more closely match the target with regard to the d
321 statistic.

322 This a greedy optimization algorithm, as it searches for only local improvements (i.e., by
323 replacing only one ground motion at a time), and thus misses opportunities for improvements
324 resulting from replacing two or more ground motions that cause an improvement in aggregate (if
325 the improvement was not detectable when replacing them one at a time). While such
326 opportunities surely exist, it is not clear that considering them would result in dramatically
327 improved selection results. Further, this choice to use a greedy optimization approach makes the
328 calculation computationally tractable. The optimization algorithm can terminate early if the error
329 metrics of equations 7 and 8 are within tolerance.

330 Once a final set of ground motions is determined, in Step 8 of Figure 2 an output file is
331 produced to document the selected ground motions (and scale factors, if scaling was allowed).
332 For the NGA-West1 and simulated ground motions, the ground motion time series are available
333 for direct download over the Internet and the selected motions' URLs are provided in the output
334 so that the time series can be obtained automatically. For the NGA-West2 database, the index
335 numbers of the selected ground motions must be copied into the NGA-West2 search tool in order
336 to download the ground motion files. Additional detail regarding this download process is
337 provided in the software documentation.

338 **4 COMPUTATIONAL EXPENSE**

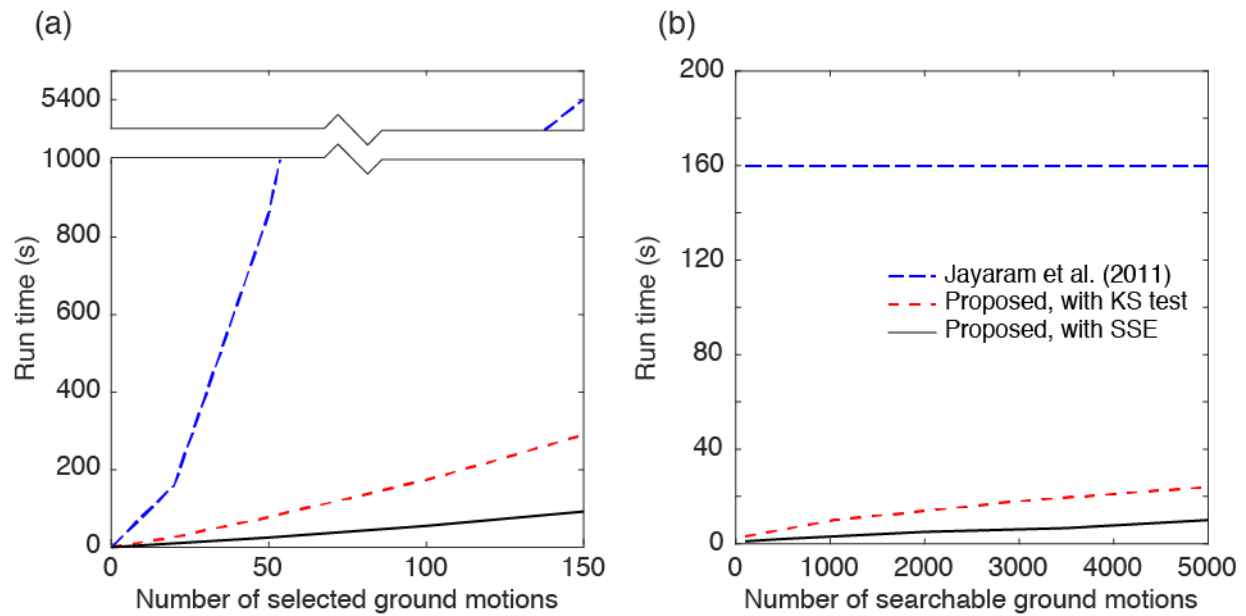
339 The algorithm's initial record-by-record selection (Step 5) takes time proportional to $m \times n$,
340 where m is the number of candidate ground motions in the database and n is the number of
341 selected ground motions, because the m motions are compared once each to the n simulations.
342 The optimization (Step 7) also takes time proportional to $m \times n$, because the $m-n$ candidates are
343 evaluated as candidates to replace each of the n previously selected motions. This is much better
344 than the m -choose- n computational expense of the exhaustive search discussed in section 2.2.
345 Any calculations within the loops over the $m \times n$ candidate evaluations were optimized to limit
346 computational cost to the extent possible.

347 We further manage computational expense in a few ways. First, we screen the database (Step
348 4 in Figure 2) to limit the size of m before starting the search for motions to select. While this is
349 conceptually simple, it was not implemented in the Jayaram et al. (2011) software. Second,
350 within the optimization stage, we skip all ground motions that need to be scaled by a larger-than-

351 allowable factor, before proceeding to the more expensive calculation of considering the ground
352 motion as a potential replacement for a currently selected motion. These first two steps often lead
353 to great reductions in the numbers of considered ground motions when typical restrictions on
354 acceptable ground motions and scale factors are used. Third, we stop the optimization early if a
355 selected set of ground motions is sufficiently close to the target spectrum (as evaluated using a
356 user-specified error tolerance). Finally, the optimization step of the algorithm—the most
357 expensive step—is optionally parallelized so that each currently selected ground motion is
358 evaluated in parallel to see if a better alternative can be found.

359 The computational cost of the algorithm is illustrated in Figure 4, for varying sizes of
360 selected ground motion sets and varying sizes of the database being searched. A few
361 observations can be made. First, the improvements discussed here have greatly reduced the
362 algorithm’s run time relative to the previous implementation by Jayaram et al. (2011). A
363 somewhat typical problem of selecting 20 ground motions from a pool of 2000 candidates now
364 requires less than 30 seconds. Second, the cost of the algorithm now scales approximately
365 linearly with the number of selected ground motions (Figure 4a) and the number of searchable
366 ground motions (Figure 4b), as expected based on the discussion above.

367 The Figure 4 results are produced without allowing early termination of the optimization and
368 without parallelized optimization, in order to provide conservative run times, so users may find
369 better performance depending upon their use of these features. The benefits of these features are
370 problem dependent, so no general run time results are provided here. Further speed-up of the
371 algorithm is possible, most obviously by switching to a faster programming language, and by
372 restructuring some code for better numerical performance. We consider the current
373 implementation to be well suited, however, for our goals of providing an educational code with
374 reasonable run times.



375
 376 Figure 4. (a) Time to select a given number of ground motions from a database of 5000 motions, for three
 377 different selection approaches. (b) Time to select 20 ground motions from a database of 5000, with
 378 varying numbers of motions remaining after screening.

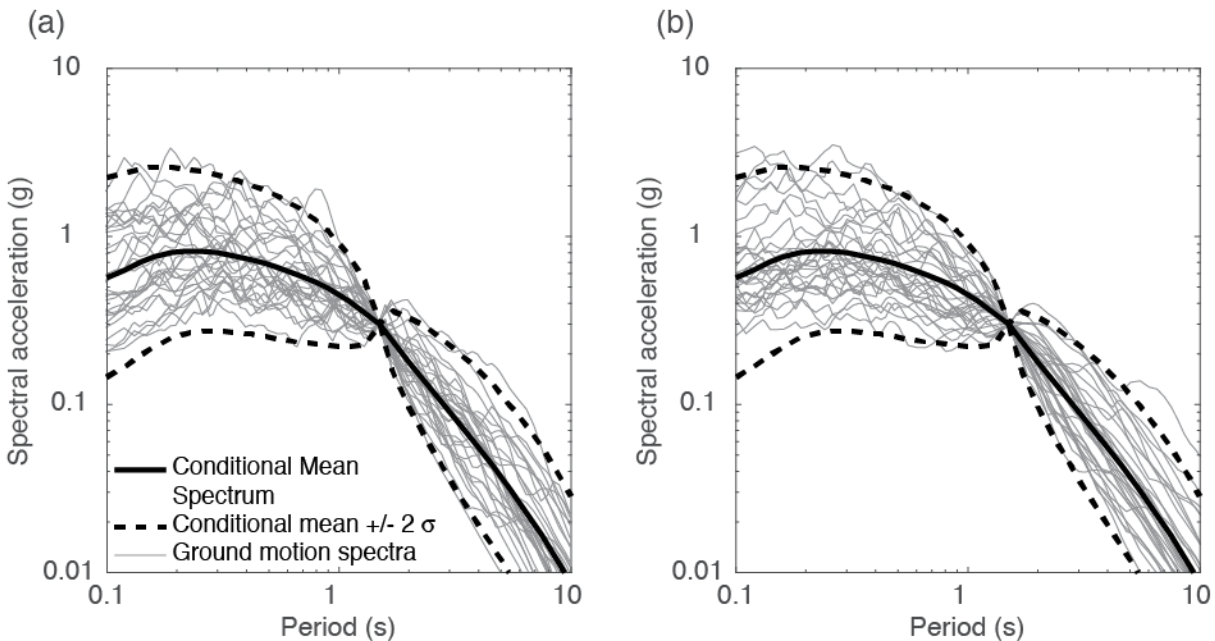
379 5 Example Ground Motion Selection

380 To illustrate use of the software, selection of simulated and recorded motions is briefly
 381 demonstrated, referring to the numbered steps in Figure 2. In step 1, the target spectrum must be
 382 specified; the Conditional Spectrum of Figure 1b is used here as the target RotD50 spectrum.
 383 Step 2 statistically simulates realizations of spectra from this distribution, and no user choices
 384 need to be made. In step 3, the ground motion database must be specified; here we consider two
 385 alternatives—the NGA-West1 database of recorded ground motions and the Graves and Pitarka
 386 database of simulated motions discussed above. In step 4 these databases are screened for
 387 suitable ground motions. In this case, because the target spectrum is associated with a magnitude
 388 = 6.5, distance = 10 km event, we restricted selection to consider only ground motions within 50
 389 km of an earthquake with magnitude between 6 and 7. Scaling of ground motions was allowed,
 390 but scale factors were limited to a maximum of five. These criteria are somewhat consistent with
 391 typical ground motion selection procedures (e.g., NIST 2011), but are used here simply to
 392 illustrate the selection process and are not recommended values. With these criteria, the NGA-
 393 West1 database had 582 ground motions satisfying the initial screening, and the GP database had
 394 6000.

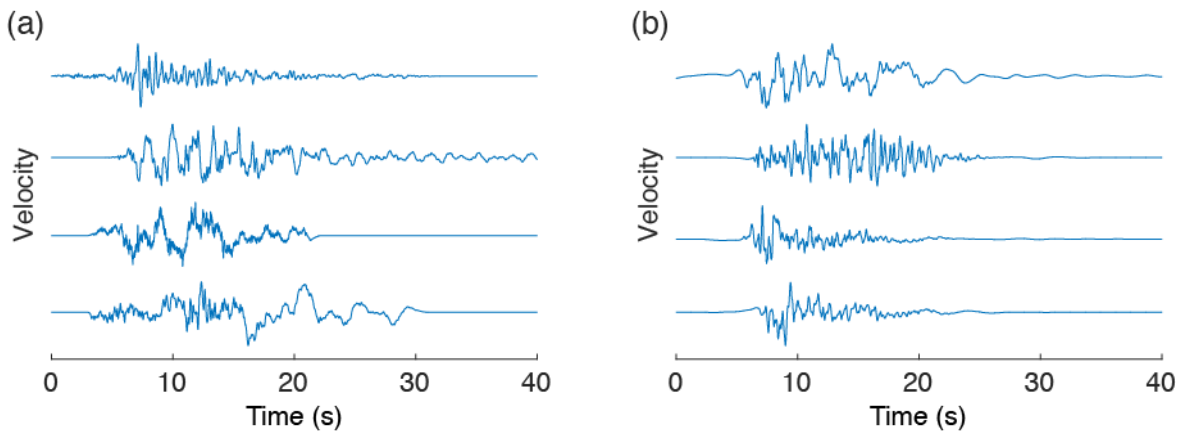
395 With the initial criteria and database screening performed, ground motions can then be
 396 selected. In step 5, initial ground motions were selected from each database to match simulated

397 spectra—a step which requires no user choices. In step 6, a maximum 10% error in means and
 398 standard deviations of the spectral was specified. Neither database satisfied that criterion with the
 399 initial selection (the step 6 check), so optimization (step 7) was performed in both cases. The
 400 SSE objective function of equation 9 was chosen for the optimization. For the NGA-West1
 401 database, the max errors in mean and standard deviation were 8% and 34%, respectively, before
 402 optimization and 6% and 7% after. For the Graves and Pitarka database, the max errors were
 403 41% and 32% before optimization and 29% and 26% after.

404 In step 8, the final selections of ground motions are output. Figure 5 shows the response
 405 spectra of the selected motions. We see that, although the Graves and Pitarka selection had
 406 significantly worse error metrics in the previous paragraph, the response spectra plot does not
 407 indicate serious deficiencies in general (the periods with poor metrics are the short periods at the
 408 left of Figure 5b); these errors would need to be evaluated on a project-specific basis for
 409 acceptability. Figure 6 shows example velocity time series for both sets of selected motions. The
 410 two sets of selected motions' time series are comparable under a cursory visual inspection. These
 411 two sets of ground motions would provide useful inputs for a more detailed study of any subtler
 412 differences in the recordings and simulations that lead them to produce different structural
 413 responses when used as input to a dynamic analysis problem. Such a study is beyond the scope
 414 of this paper but is the type of exercise that the new software features are intended to facilitate.



415
 416 Figure 5. Response spectra of selected ground motions with spectra matching the target Conditional
 417 Spectrum of Figure 1b. The mean and mean +/- two standard deviations of the target $\ln Sa$ distribution are
 418 superimposed. (a) NGA-West1 recorded ground motions. (b) Graves and Pitarka simulated ground
 419 motions.



420
421

422 Figure 6. Example velocity time series from the selected motions shown in Figure 5. The time series are
423 scaled to have the same peak ground velocity values for ease of comparison, so no velocity scale is
424 provided. (a) NGA-West1 recorded ground motions. (b) Graves and Pitarka simulated ground motions.

425 6 Numerical Implementation

426 Matlab source code for the algorithm is available at
427 https://github.com/bakerjw/CS_Selection. The repository includes metadata and documentation
428 for five ground motion databases discussed above. In addition to the algorithmic features
429 discussed above, this source code also improves upon the previous code from Jayaram et al.
430 (2011) by providing a single general purpose program (the Jayaram et al. code consistent of four
431 separate programs for conditional versus unconditional selection, and single-component versus
432 two-component selection), and better modularization of functions related to the tasks outlined in
433 Figure 2.

434 7 Conclusions

435 This paper has presented an efficient algorithm for selecting ground motions from a database
436 that match a target response spectrum distribution (i.e., a Conditional Spectrum or Unconditional
437 Spectrum). The motivation for this work is that when the target spectrum has a distribution,
438 rather than a single value, it is not possible to evaluate individual ground motions for selection
439 without considering them as part of a suite of ground motions that collectively represent the
440 distribution. But evaluating all possible suites of ground motions is impossible when considering
441 large ground motion databases typical in practice today. This algorithm utilizes several heuristics
442 to quickly identify ground motion sets with close match to the target spectrum.

443 Note that the code can also be easily adapted for the more common situation where the user
444 wants to select ground motions that each closely match a target spectrum (e.g., for closely

445 matching a design spectrum from a building code, with each motion closely matching the target)
446 by specifying the target spectrum as the mean value and setting the target variances to zero. The
447 algorithm's complexity is more than is needed for this simpler application, but it is well-suited
448 for the problem and so a user-defined flag setting the variance to zero is provided in the software.

449 The key steps in this algorithm are (1) compute a target response spectrum distribution, (2)
450 statistically simulate response spectra from the target distribution, (3) load and screen a database
451 of candidate ground motions, (4) select ground motions from the database that individually
452 match the statistically simulated spectra, (5) make incremental changes to the initially selected
453 ground motion set to further optimize its fit to the target spectrum distribution. The algorithm
454 follows the general structure of a proposal by Jayaram et al. (2011), but incorporates a number of
455 new features that improve its utility and speed.

456 Data for a number of new ground motion databases are also provided, to allow users to
457 search recently developed catalogs of recorded or simulated ground motion data. Example
458 selection of comparable recorded and simulated ground motions are illustrated, to demonstrate
459 the feasibility of selecting equivalent motions from differing sources. Matlab source code for the
460 algorithm has been provided publically for readers interested in using or modifying the
461 algorithm.

462 **Acknowledgements**

463 We thank Nenad Bijelic, Reagan Chandramohan, Beliz Ugurhan and three anonymous
464 reviewers for helpful advice and comments on this work. This work was supported in part by the
465 State of California through the Transportation Systems Research Program of the Pacific
466 Earthquake Engineering Research Center (PEER).

467 **References**

- 468 Abrahamson, N. A., and Al Atik, L. (2010). "Scenario Spectra for Design Ground Motions and
469 Risk Calculation." *9th US National and 10th Canadian Conference on Earthquake
470 Engineering*, Toronto, Canada, 12.
- 471 Abrahamson, N. A., Silva, W. J., and Kamai, R. (2014). "Summary of the ASK14 Ground
472 Motion Relation for Active Crustal Regions." *Earthquake Spectra*, 30(3), 1025–1055.
- 473 Ancheta, T. D., Darragh, R. B., Stewart, J. P., Seyhan, E., Silva, W. J., Chiou, B. S.-J.,
474 Wooddell, K. E., Graves, R. W., Kottke, A. R., Boore, D. M., Kishida, T., and Donahue,
475 J. L. (2014). "NGA-West2 Database." *Earthquake Spectra*, 30(3), 989–1005.
- 476 Atkinson, G. M., and Assatourians, K. (2015). "Implementation and validation of EXSIM (a
477 stochastic finite-fault ground-motion simulation algorithm) on the SCEC broadband
478 platform." *Seismological Research Letters*, 86(1), 48–60.

479 Baker, J. W. (2011). "Conditional Mean Spectrum: Tool for ground motion selection." *Journal*
480 *of Structural Engineering*, 137(3), 322–331.

481 Baker, J. W., and Cornell, C. A. (2006). "Spectral shape, epsilon and record selection." *Earthquake Engineering & Structural Dynamics*, 35(9), 1077–1095.

482 Baker, J. W., and Jayaram, N. (2008). "Correlation of spectral acceleration values from NGA
483 ground motion models." *Earthquake Spectra*, 24(1), 299–317.

484 Beyer, K., and Bommer, J. J. (2007). "Selection and Scaling of Real Accelerograms for Bi-
485 Directional Loading: A Review of Current Practice and Code Provisions." *Journal of*
486 *Earthquake Engineering*, 11, 13–45.

487 Boore, D. M. (2010). "Orientation-Independent, Nongeometric-Mean Measures of Seismic
488 Intensity from Two Horizontal Components of Motion." *Bulletin of the Seismological*
489 *Society of America*, 100(4), 1830–1835.

490 Boore, D. M., Stewart, J. P., Seyhan, E., and Atkinson, G. M. (2014). "NGA-West2 Equations
491 for Predicting PGA, PGV, and 5% Damped PSA for Shallow Crustal Earthquakes." *Earthquake Spectra*, 30(3), 1057–1085.

492 Bradley, B. A. (2010). "A generalized conditional intensity measure approach and holistic
493 ground-motion selection." *Earthquake Engineering & Structural Dynamics*, 39(12),
494 1321–1342.

495 Bradley, B. A. (2012). "A ground motion selection algorithm based on the generalized
496 conditional intensity measure approach." *Soil Dynamics and Earthquake Engineering*,
497 40, 48–61.

498 BSSC. (2015). *NEHRP Recommended Seismic Provisions for New Buildings and Other*
499 *Structures*. FEMA P-1050, Building Seismic Safety Council, Washington, D.C., 515p.

500 Buratti, N., Stafford, P. J., and Bommer, J. J. (2010). "Earthquake Accelerogram Selection and
501 Scaling Procedures for Estimating the Distribution of Drift Response." *Journal of*
502 *Structural Engineering*, 137(3), 345–357.

503 Chandramohan, R., Baker, J. W., and Deierlein, G. G. (2016). "Impact of hazard-consistent
504 ground motion duration in structural collapse risk assessment." *Earthquake Engineering*
505 *and Structural Dynamics*, (in press).

506 Chiou, B., Darragh, R., Gregor, N., and Silva, W. (2008). "NGA Project Strong-Motion
507 Database." *Earthquake Spectra*, 24(1), 23–44.

508 FEMA. (2012). *Seismic Performance Assessment of Buildings*. FEMA P-58, Prepared by
509 Applied Technology Council for the Federal Emergency Management Agency.

510 Galasso, C., Zhong, P., Zareian, F., Iervolino, I., and Graves, R. W. (2013). "Validation of
511 ground-motion simulations for historical events using MDoF systems." *Earthquake*
512 *Engineering & Structural Dynamics*, 42(9), 1395–1412.

513 Goulet, C. A., Abrahamson, N. A., Somerville, P. G., and Wooddell, K. E. (2015). "The SCEC
514 Broadband Platform Validation Exercise: Methodology for Code Validation in the
515 Context of Seismic - Hazard Analyses." *Seismological Research Letters*, 86(1), 17–26.

516 Graves, R., and Pitarka, A. (2015). "Refinements to the Graves and Pitarka (2010) Broadband
517 Ground - Motion Simulation Method." *Seismological Research Letters*, 86(1), 75–80.

518 Ha, S. J., and Han, S. W. (2016a). "A method for selecting ground motions that considers target
519 response spectrum mean and variance as well as correlation structure." *Journal of*
520 *Earthquake Engineering*, (in press).

521 Ha, S. J., and Han, S. W. (2016b). "An efficient method for selecting and scaling ground motions
522 matching target response spectrum mean and variance." *Earthquake Engineering &*
523 *Structural Dynamics*, 45(8), 1381–1387.

526 Iervolino, I., De Luca, F., and Cosenza, E. (2010). "Spectral shape-based assessment of SDOF
527 nonlinear response to real, adjusted and artificial accelerograms." *Engineering Structures*,
528 32(9), 2776–2792.

529 Jayaram, N., and Baker, J. W. (2008). "Statistical Tests of the Joint Distribution of Spectral
530 Acceleration Values." *Bulletin of the Seismological Society of America*, 98(5), 2231–
531 2243.

532 Jayaram, N., Lin, T., and Baker, J. W. (2011). "A computationally efficient ground-motion
533 selection algorithm for matching a target response spectrum mean and variance." *Earthquake Spectra*, 27(3), 797–815.

534 Katsanos, E. I., Sextos, A. G., and Manolis, G. D. (2010). "Selection of earthquake ground
535 motion records: A state-of-the-art review from a structural engineering perspective." *Soil
536 Dynamics and Earthquake Engineering*, 30(4), 157–169.

537 Kottke, A., and Rathje, E. M. (2008). "A Semi-Automated Procedure for Selecting and Scaling
538 Recorded Earthquake Motions for Dynamic Analysis." *Earthquake Spectra*, 24(4), 911–
539 932.

540 Kramer, S. L., and Mitchell, R. A. (2006). "Ground Motion Intensity Measures for Liquefaction
541 Hazard Evaluation." 22(2), 413–438.

542 Lin, T., Harmsen, S. C., Baker, J. W., and Luco, N. (2013a). "Conditional Spectrum
543 Computation Incorporating Multiple Causal Earthquakes and Ground Motion Prediction
544 Models." *Bulletin of the Seismological Society of America*, 103(2A), 1103–1116.

545 Lin, T., Haselton, C. B., and Baker, J. W. (2013b). "Conditional spectrum-based ground motion
546 selection. Part I: Hazard consistency for risk-based assessments." *Earthquake
547 Engineering & Structural Dynamics*, 42(12), 1847–1865.

548 NIST. (2011). *Selecting and Scaling Earthquake Ground Motions for Performing Response-
549 History Analyses*. NIST GCR 11-917-15, Prepared by the NEHRP Consultants Joint
550 Venture for the National Institute of Standards and Technology, Gaithersburg, Maryland.

551 Olsen, K., and Takedatsu, R. (2015). "The SDSU Broadband Ground-Motion Generation
552 Module BBtoolbox Version 1.5." *Seismological Research Letters*, 86(1), 81–88.

553 Stein, M. (1987). "Large Sample Properties of Simulations Using Latin Hypercube Sampling." *Technometrics*, 29(2), 143–151.

554 Stewart, J. P., Abrahamson, N. A., Atkinson, G. M., Baker, J. W., Boore, D. M., Bozorgnia, Y.,
555 Campbell, K. W., Comartin, C. D., Idriss, I. M., Lew, M., Mehrain, M., Moehle, J. P.,
556 Naeim, F., and Sabol, T. A. (2011). "Representation of Bi-Directional Ground Motions
557 for Design Spectra in Building Codes." *Earthquake Spectra*, 27(3), 927–937.

558 Tarbali, K., and Bradley, B. A. (2016). "The effect of causal parameter bounds in PSHA-based
559 ground motion selection." *Earthquake Engineering & Structural Dynamics*, (in press).

560 TBI Guidelines Working Group. (2010). "Guidelines for performance-based seismic design of
561 tall buildings." *Berkeley: University of California (PEER Report No. 2010/05)*.

562 Wang, G. (2011). "A ground motion selection and modification method capturing response
563 spectrum characteristics and variability of scenario earthquakes." *Soil Dynamics and
564 Earthquake Engineering*, 31(4), 611–625.

565
566
567